

# Journal of Materials Chemistry A

Accepted Manuscript



This is an *Accepted Manuscript*, which has been through the Royal Society of Chemistry peer review process and has been accepted for publication.

*Accepted Manuscripts* are published online shortly after acceptance, before technical editing, formatting and proof reading. Using this free service, authors can make their results available to the community, in citable form, before we publish the edited article. We will replace this *Accepted Manuscript* with the edited and formatted *Advance Article* as soon as it is available.

You can find more information about *Accepted Manuscripts* in the [Information for Authors](#).

Please note that technical editing may introduce minor changes to the text and/or graphics, which may alter content. The journal's standard [Terms & Conditions](#) and the [Ethical guidelines](#) still apply. In no event shall the Royal Society of Chemistry be held responsible for any errors or omissions in this *Accepted Manuscript* or any consequences arising from the use of any information it contains.

## ARTICLE

# Bipolar Anodization Enables the Fabrication of Controlled Arrays of TiO<sub>2</sub> Nanotube Gradients

Cite this: DOI: 10.1039/x0xx00000x

G. Loget,<sup>a</sup> S. So,<sup>a</sup> R. Hahn<sup>a</sup> and P. Schmuki<sup>a,b\*</sup>

Received 00th January 2012,

Accepted 00th January 2012

DOI: 10.1039/x0xx00000x

[www.rsc.org/](http://www.rsc.org/)

We report here a new concept, the use of bipolar electrochemistry, which allows the rapid and wireless growth of self-assembled TiO<sub>2</sub> NT layers that consist of highly defined and controllable gradients in NT length and diameter. The gradient height and slope can be easily tailored with the time of electrolysis and the applied electric field, respectively. As this technique allows obtaining in one run a wide range of self-ordered TiO<sub>2</sub> NT dimensions, it provides the basis for rapid screening of TiO<sub>2</sub> NT properties. In two examples, we show how these gradient arrays can be used to screen for an optimized photocurrent response from TiO<sub>2</sub> NT based devices such as dye-sensitized solar cells.

## Introduction

Over the past decade, arrays of aligned TiO<sub>2</sub> nanotubes (TiO<sub>2</sub> NTs) grown on Ti by self-organizing anodization have attracted a huge scientific interest.<sup>1,2</sup> Due to the electronic properties and the biocompatibility of TiO<sub>2</sub>, these one-dimensional nanostructure arrays are highly promising for applications in the fields of dye-sensitized solar cells (DSSCs),<sup>1,3-4</sup> water splitting,<sup>5</sup> photocatalysis<sup>6</sup> and biomedical devices.<sup>7,8</sup> The performance of the nanotubes in all these applications depends strongly on their length, diameter and ordering. For instance, an optimal length of 7 μm for TiO<sub>2</sub> nanotubes has been reported for solar photoelectrochemical water splitting,<sup>9</sup> ranges of 15-30 μm seem optimum for DSSCs,<sup>4</sup> and it has been shown that TiO<sub>2</sub> nanotubes with a diameter larger than 50 nm impaired the spreading and adhesion of mesenchymal stem cells on nanotubular surfaces.<sup>7,10</sup> Screening the properties of TiO<sub>2</sub> NT arrays as a function of the tubes characteristic dimensions for a given

application is consequently of significant importance for the development and the optimization of many important TiO<sub>2</sub> NT-based devices. In the majority of the cases, screening requires fabricating and studying series of individual surfaces, each of them comprised of one type of nanotubes with a specific characteristic tube dimension, this approach is time consuming and expensive. Therefore, it would be beneficial to develop a reliable and efficient technique that allows the fabrication of TiO<sub>2</sub> NT arrays with adjustable length and diameter gradients for the rapid screening of these factors on a single sample. In the present work we show that such gradients can be generated in a highly controlled manner using bipolar electrochemistry.

Bipolar electrochemistry is a phenomenon which generates redox reactions on the surface of conductive objects without the use of wires.<sup>13</sup> It has recently attracted considerable attention for micro- and nanosciences with applications in the domains of analysis,<sup>14</sup> materials science,<sup>15</sup> as well as for the generation of particle motion.<sup>16</sup> Although bipolar electrochemistry can be conceived as a straightforward fabrication technique of various

potential induced surface gradients, only a few papers describe its use for this purpose. Björefors *et al.* used bipolar electrochemistry-triggered desorption of self-assembled monolayers for the formation of molecular gradients on gold,<sup>17</sup> Shannon *et al.* reported the bipolar electrodeposition for the fabrication of Au-Ag and CdS solid-state gradients,<sup>18</sup> and Inagi and Fuchigami used bipolar doping to fabricate gradually-doped conducting polymers.<sup>19</sup> In the present paper, we combine for the first time anodization and bipolar electrochemistry in order to fabricate in a few minutes and in a wireless manner self-assembled TiO<sub>2</sub> NT surfaces, which are comprised of NT gradients with tunable length and diameter and we show how these gradients can be used for the rapid screening of the TiO<sub>2</sub> NT properties.

## Principle and mechanism

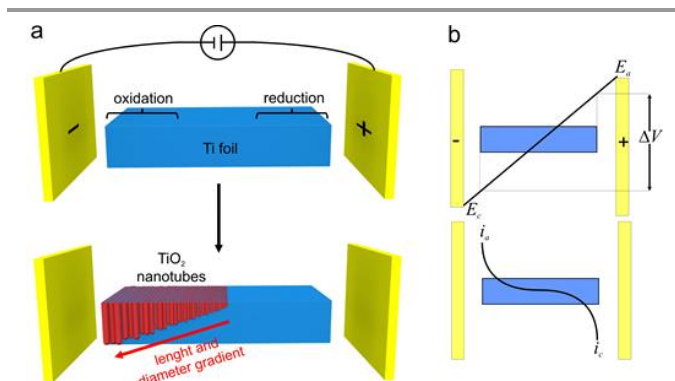


**Fig. 1.** a) Scheme showing the principle of bipolar anodization. The Ti foil becomes a bipolar electrode under a sufficiently high electric field, which leads to the formation of a gradient of TiO<sub>2</sub> NTs at its anodic pole. b) Scheme showing the polarization potential distribution (top) and the faradaic current distribution (bottom) on a bipolar electrode.<sup>†</sup>

Fig. 1 illustrates the principle of bipolar anodization. First, a Ti foil located between two feeder electrodes lies in the electrolyte with no direct electrical connection. When an electric field is applied between the feeder electrodes, namely an anode at a potential  $E_a$  and a cathode at a potential  $E_c$ , a polarization potential  $\Delta V$  arises along the surface of the Ti foil.<sup>13</sup> As shown in Fig. 1b, this potential is maximal at the edges of the foil and gradually decreases towards its middle. If the generated polarization potential is high enough, a fraction of the delivered current flows through the Ti foil, inducing redox reactions along the metal conducting path but most pronounced at its extremities, where the polarization potential is

maximum.<sup>13</sup> Reduction happens at the cathodic pole of the Ti foil (the extremity which faces the feeder anode), together with oxidation at the anodic pole (extremity which faces the feeder cathode). Under such conditions the Ti foil behaves at the same time as an anode and a cathode, that is a bipolar electrode. Since the driving force of the electrochemical reaction,  $\Delta V$ , gradually decreases from the edge of the reactive pole towards the middle of the foil, this mechanism, performed under appropriate anodization conditions, should allow to grow TiO<sub>2</sub> NTs with a length and diameter gradient on the anodic pole.

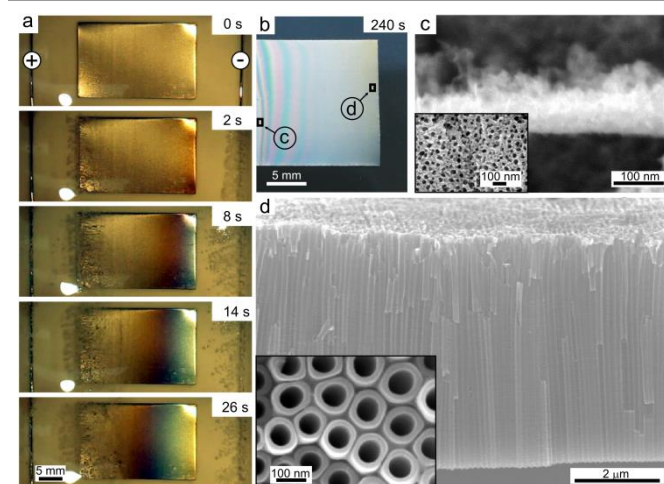


**Fig. 2.** a) Series of photographs showing the first 26 s of a bipolar anodization experiment. b) Photograph of the anodic pole of the Ti foil after 240 s of bipolar anodization. c) SEM cross-section of the oxide layer located at spot c in Fig. 2b. Inset: SEM top view of the layer. d) SEM cross-section of layer located at spot d in Fig. 2b. Inset: SEM picture showing the sections of TiO<sub>2</sub> NTs.

Fig. 2 and video 1 (provided in supplementary information) show a proof-of-principle experiment in which a 2.5 cm-long Ti foil immersed in an ethylene glycol-based electrolyte containing lactic acid (recently developed in our lab for the ultrafast growth of ordered TiO<sub>2</sub> NTs)<sup>20</sup> was polarized by a 37 V.cm<sup>-1</sup> electric field. At 2 s, the color of the anodic pole became brownish due to the formation of a titanium oxide layer interfering with some wavelengths of the visible light.<sup>21</sup> Simultaneously bubble evolution occurred at the opposite edge (the cathodic pole) of the foil, caused by the reduction of the electrolyte. Over time the colored front extended towards the cathodic pole, together with the emergence of a linear interference color gradient (from brown to white) caused by the thickness increase of the Ti oxide layer over the surface (thickness =  $f_{ox} U_x$  with  $f_{ox}$  = oxide growth rate and  $U_x$  is the

local effective potential at a given surface location) Fig. 2b shows the anodic pole of the Ti foil after 4 min of anodization. The oxide layer, mostly greyish, covered more than 60 % of the Ti foil surface. Scanning electron microscope (SEM) observations were performed at the two extremities of the anodic pole. A porous oxide layer (Fig. 2c) with a thickness of about 100 nm and non-organized nanopores (Fig. 2c, inset), was observed at the edge which underwent the weakest polarization potential. In contrast, as shown in Fig. 2d, the opposite edge, which underwent the highest polarization potential, carried a 5.5  $\mu\text{m}$ -thick layer composed of self-organized  $\text{TiO}_2$  NTs. The presence of such  $\text{TiO}_2$  NT layer over the anodic pole suggest that the anodic reactions happening on this area during polarization involve the oxidation of the metal Ti surface to form  $\text{TiO}_2$  and soluble  $\text{Ti}^{4+}$  complexes with fluoride, as it is the case for conventional electrochemical formation of  $\text{TiO}_2$  NTs.<sup>1</sup> This proof-of-principle experiment shows that bipolar anodization can be used for the fabrication of oxide layers with different thicknesses on one Ti foil, but more importantly also layers of self-organized  $\text{TiO}_2$  NT arrays can be formed. We demonstrate in the following examples that the concept of bipolar anodization can be used for the straightforward, rapid and reliable fabrication of  $\text{TiO}_2$  NT dimensional gradients.

### Control over the distribution of the nanotube lengths and diameters

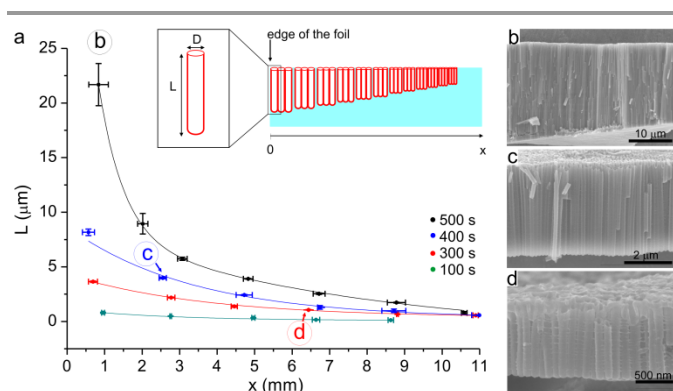


**Fig. 3.** a) Curves showing the evolution of  $L$  as a function of  $x$  for different bipolar anodization times using a  $55 \text{ V.cm}^{-1}$  electric field. Inset: scheme of a  $\text{TiO}_2$  NT gradient varying along the  $x$  axis and characteristic dimensions of a single tube, namely length  $L$  and diameter  $D$ . b), c) and d) SEM pictures showing cross-sections of the oxide layers respectively obtained at the b, c and d points of Fig. 3a.

The inset of Fig. 3a defines the position  $x$  on the Ti foil as well as the characteristic dimensions of single NTs, length  $L$  and diameter  $D$ . Fig. 3b shows gradients obtained after imposing an electric field of  $E = 55 \text{ V.cm}^{-1}$  on 1.8 cm-long Ti foils for different times (a detailed description of the electrochemical cell is provided in Fig. S1). First, it is clear that in every case the longest  $\text{TiO}_2$  NTs were obtained at the edge of the anodic pole and their length decreased in the direction of the other edge of the foil. The length decrease is found of an exponential nature which suggests a correlation between  $L$  and the current distribution and that the anodization reaction is not limited by mass transfer because the current distribution over a bipolar electrode (see Fig. 1b) follows the exponential Butler-Volmer relationship in the case of electron-transfer limited reaction.<sup>14,22,23</sup> A very useful finding is that the height of the gradient can be easily tuned by the charge passed through the bipolar electrode, thus, simply by the time of the electrolysis. As shown in these graphs, the longest tubes ( $L \approx 22 \mu\text{m}$ ) were obtained for an electrolysis time of 500 s. At this position, the  $L$  gradient can easily be seen in the cross-section SEM of Fig. 3c. The smallest measured tubes, obtained with an electrolysis time of 100 s, were shorter than 500 nm. These results show that  $\text{TiO}_2$  NT length gradients can be easily fabricated and tuned by bipolar anodization.

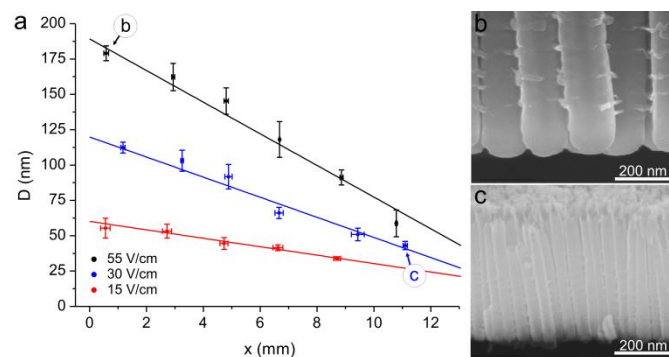


**Fig. 4.** a) Curves showing the evolution of diameter  $D$  as a function of  $x$  for different applied electric fields. b) and c) SEM pictures showing the  $\text{TiO}_2$  NTs respectively obtained at the b and c points of Fig. 4a.

The tube diameters were not significantly affected by the time of electrolysis (see Fig. S6) but directly by the applied electric field, as shown in Fig. 4. The bipolar anodizations performed for this figure were performed at three different electric fields: 55, 30 and  $15 \text{ V.cm}^{-1}$ . As the growth rate decreased with decreasing electric field values, the electrolysis

was performed during a longer time ( $t = 4, 14$  and  $75$  min, respectively). The  $D$  gradient curves, shown in Fig. 4, demonstrate that the evolution of  $D$  as a function of the position  $x$  is linear over the anodic pole, which suggest that it is controlled by the variation of the polarization potential over the anodic pole (see Fig. 1b).<sup>13</sup> This is consistent with the fact that the  $D$  gradient is adjustable with the applied electric field because the polarization potential is proportional to the imposed electric field.<sup>13</sup> The largest tubes, shown in Fig. 4b, had a diameter of  $180$  nm and were obtained for  $E = 55$  V.cm<sup>-1</sup>. In this case the ratio  $D_{\text{max}}/D_{\text{min}} = 3$  with a slope of  $11.2$  nm.mm<sup>-1</sup>. The narrowest measured tubes had a diameter smaller than  $35$  nm and were obtained with  $E = 15$  V.cm<sup>-1</sup> (slope =  $3.0$  nm.mm<sup>-1</sup>). These results illustrate that TiO<sub>2</sub> NTs also with a gradient in diameter can be easily fabricated and tailored using bipolar anodization.

### Photocurrent screening

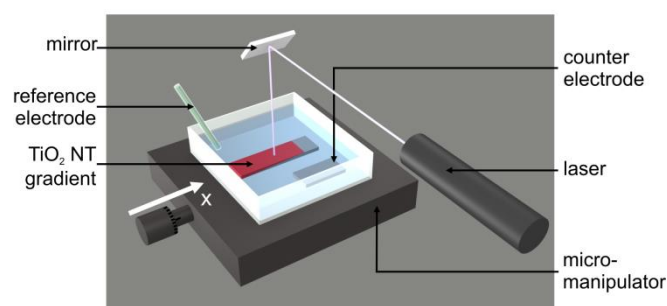


Fig. 5. Scheme of the set-up used for photocurrent screening.

After having shown the fabrication of TiO<sub>2</sub> NT gradients, we now demonstrate two examples how they can be used for the fast screening of the NT properties. Motivated by the current scientific discussion in the literature about the optimal characteristic tube dimensions that provide a maximum photoresponse e.g. in photocatalysis or DSSCs,<sup>4,6,9</sup> we screened our gradients in a photoelectrochemical set-up, as illustrated in Fig. 5.

The gradients used in these experiments were fabricated by bipolar anodization on  $3.8 \times 1$  cm Ti foils (see supporting information for experimental details). As shown in Fig. 6b, those surfaces comprised  $2.4$  cm-long TiO<sub>2</sub> NT gradients with a ratio between the maximum and minimum length values  $L_{\text{max}}/L_{\text{min}} \approx 100$ . The gradients were annealed to anatase form

(see Fig. S4 for X-ray diffraction spectrum) and placed in the photoelectrochemical cell (experimental details are given in supporting information). This cell consisted of a Ag/AgCl reference electrode, a Pt counter electrode and the TiO<sub>2</sub> NT gradient foil, used as a working electrode. The cell was filled with the electrolyte and a potentiostat was used for applying a potential to the tube gradient electrode ( $+500$  mV vs Ag/AgCl) and for recording currents. A UV light spot, with a diameter of  $1.5$  mm (FWHM of the Gaussian intensity distribution), generated by a HeCd laser ( $325$  nm) was used for illuminating the gradient locally. A micromanipulator, mounted below the cell, was used for moving the cell and thus scanning the gradient along its  $x$  axis. A dark current  $I_d \approx 2$   $\mu$ A was measured and the transient currents were recorded while imposing  $10$  s pulses with the laser for different  $x$  values, as shown in the inset of Fig. 6a.

Fig. 6a shows the photocurrent profile along the gradient. From this curve it is clear that the minimum photocurrents (with  $I_{\text{min}} = 0.3$  mA) were obtained for lower  $x$  value, the values then increased, to a value  $I_{\text{max}} = 1.53$  mA for  $x = 14$  mm and decreased down to a value of  $1.06$  mA for increasing  $x$  values. The plots of the photocurrent as a function of the TiO<sub>2</sub> NT length and diameter, shown in Fig. 6c, reveal that the highest photocurrent were obtained for  $L = 6$   $\mu$ m and  $D = 108$  nm. These results are in very good agreement with previous published works.<sup>9</sup> It is also worth mentioning that the transient photocurrent curves obtained with the longest tubes exhibited a decay after illumination (Inset of Figure 6a), this can be attributed to an increased recombination over longer transport pathways. The experiment demonstrates the feasibility to use these gradients for the fast screening of tube properties over a wide range of dimensions.

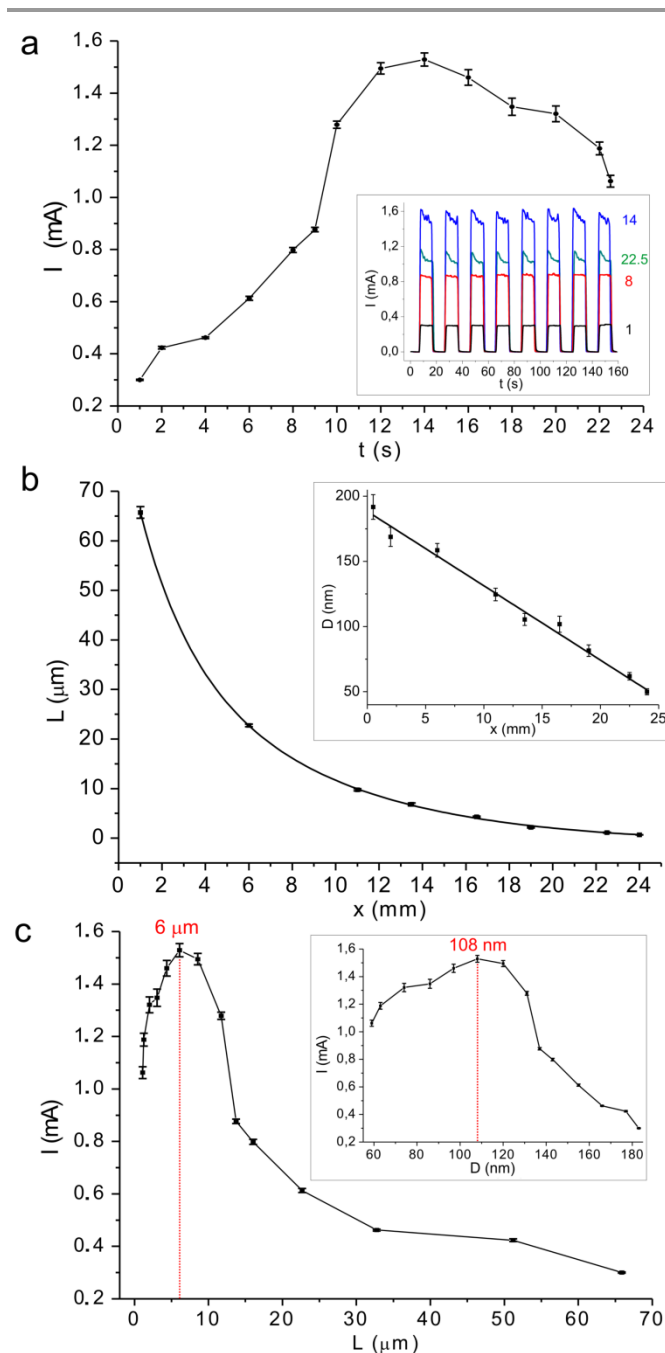


**Fig. 6.** a) Curve showing the photocurrent evolution as a function of  $x$ . Inset: transient photocurrent curves for 4 different positions on the gradient ( $x = 1, 7, 14$  and  $22.5$  mm). b) Length distribution over the TiO<sub>2</sub> NT gradient. Inset: diameter distribution over the TiO<sub>2</sub> NT gradient. c) Curve showing the photocurrent evolution as a function of  $L$ . Inset: Curve showing the photocurrent evolution as a function of  $D$ .

## Determination of the optimal dimensions of dye-sensitized TiO<sub>2</sub> NTs

We now show a second direct application of our gradients, that can be used for optimizing TiO<sub>2</sub> NT based DSSCs. For these experiments, we used a gradient made similarly to the previously described one. After annealing, the gradient was sensitized with a ruthenium dye and the screening was performed with the set-up similar to the one previously described in Fig. 5. In this case a laser of  $\lambda = 473$  nm and an acetonitrile-based electrolyte containing the iodide/tri-iodide redox couple were used (see supplementary information, section 1-3 for experimental details). In order to avoid water contamination that could provoke dye desorption, a Pt electrode was used as a pseudo-reference electrode and +500 mV were imposed to the gradient. A dark current  $I_d \approx 7 \mu\text{A}$  was measured and the current under light irradiation was measured for different  $x$  values after 30 s of equilibrium. The photocurrent values as a function of  $x$  are shown in Fig. 7a. The maximum photocurrent  $I_{\text{max}} = 70 \mu\text{A}$  was found for  $x = 4$  mm. The TiO<sub>2</sub> NTs present at this location were observed at the SEM and are shown in Fig. 7b. The length of these tubes at  $x = 4$  mm is  $L = 30 \mu\text{m}$  with a measured diameter of  $D = 164 \pm 9$  nm, which is in very good agreement with Fig. 6b. These dimensions are in the same range than the ones reported in recent work discussing the optimal tube length for DSSCs.<sup>4</sup> The fabrication and the screening experiment was performed in a few hours whereas it would have taken much longer time using classical anodization procedures, probably several days. These results demonstrate clearly how these gradients and the described screening methods can be beneficial for rapidly optimizing photoelectrochemical devices.

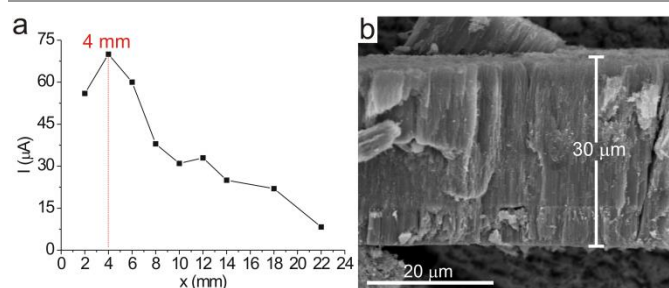


**Fig. 7.** a) Curve showing the photocurrent evolution as a function of  $x$ . b) SEM picture showing a cross-section of the oxide layer at  $x = 4$  mm.

## Conclusion

In summary, we report a new concept of bipolar anodization which allows the rapid wireless fabrication of self-organized TiO<sub>2</sub> NTs layers with a gradient in length and in diameter. The length and the diameter of the tubes are respectively correlated with the current and the potential distribution over the bipolar electrode. This makes the height of these gradients easily tunable using simple experimental parameters, such as the time of electrolysis and the applied electric field. The highest ratio between the maximum and minimum measured dimensions was about 100 and 4 for length and diameter respectively, which are the highest dimensional variations reported so far for TiO<sub>2</sub> NT gradients.<sup>11-12</sup> The application of these gradients for the fast scanning of the tube properties was demonstrated and allowed determining the optimal tube characteristics for photocurrent generation under UV light (L = 6 μm and D = 110 nm) and for dye sensitized tubes under visible light (L = 30 μm and D = 160 nm). The fabrication and the screening of those gradients could be performed in only a few hours whereas such a broad screening of tube properties performed with conventional anodization techniques would have taken at least several days. This technique thus opens up a path to rapid screening of self-ordered TiO<sub>2</sub> NT properties as a function of individual tube dimensions. For example, local photocurrents under different light sources or simulated sunlight or maximum biocompatibility can be screened straightforward; therefore the future optimization of TiO<sub>2</sub> NT-based devices in applications such as photovoltaic cells,<sup>1</sup> photoelectrochemical water splitting,<sup>5</sup> and biomedical devices<sup>7</sup> can be drastically faster.

## Acknowledgements

This work was supported by a post-doctoral research grant from the Alexander von Humboldt Foundation. ERC and DFG are acknowledged for support. Dr. Altomare, Dr. Lee and Prof. Virtanen are acknowledged for valuable discussions.

## Notes and references

<sup>a</sup> Department of Materials Science WW-4, LKO, University of Erlangen-Nuremberg, Martensstrasse 7, 91058 Erlangen (Germany)

<sup>b</sup> Department of Chemistry, King Abdulaziz University, Jeddah (Saudi Arabia)

Schmuki@ww.uni-erlangen.de

† The potential drops at the solid/liquid interfaces and the mass-transfer effects are considered negligible in these schemes. For more information, see refs. 14 and 22.

Electronic Supplementary Information (ESI) available: video 1, experimental section, characterization of the annealed gradients, screening of the experimental conditions and effect of the electrolysis time on the tube diameter.

See DOI: 10.1039/b000000x/

- 1 P. Roy, S. Berger and P. Schmuki, *Angew. Chem. Int. Ed.*, 2011, **50**, 2904. K. Lee, A. Mazare, P. Schmuki, *Chem. Rev.*, DOI: dx.doi.org/101021cr500061m
- 2 D. Kowalski, D. Kim and P. Schmuki, *Nano Today*, 2013, **8**, 235.
- 3 K. Zhu, T. B. Vinzant, N. R. Neale and A. J. Frank, *Nano Lett.*, 2007, **7**, 3739; G. K. Mor, O. K. Varghese, M. Paulose, K. Shankar and C. A. Grimes, *Sol. Energ. Mat. Sol. Cells*, 2006, **90**, 2011; J. R. Jennings, A. Ghicov, L. M. Peter, P. Schmuki, A. B. Walker, *J. Am. Chem. Soc.*, 2008, **130**, 13364.
- 4 P. Roy, D. Kim, K. Lee, E. Spiecker and P. Schmuki, *Nanoscale*, 2010, **2**, 45.
- 5 N. Liu, C. Schneider, D. Freitag, M. Hartmann, U. Venkatesan, J. Müller, E. Spiecker and P. Schmuki, *Nano Lett.*, 2014, **14**, 3309; Y. Yuxin, J. Zhengguo and H. Feng, *Nanotechnology*, 2007, **18**, 495608; P. Roy, C. Das, K. Lee, R. Hahn, T. Ruff, M. Moll and P. Schmuki, *J. Am. Chem. Soc.*, 2011, **133**, 5629.
- 6 Y.-Y. Song, F. Schmidt-Stein, S. Bauer and P. Schmuki, *J. Am. Chem. Soc.*, 2009, **131**, 4230. W.-T. Sun, Y. Yu, H.-Y. Pan, X.-F. Gao, Q. Chen and L.-M. Peng, *J. Am. Chem. Soc.*, 2008, **130**, 1124; A. Fujishima, X. Zhang and D. A. Tryk, *Surf. Sci. Rep.*, 2008, **63**, 515; I. Paramasivam, H. Jha, N. Liu and P. Schmuki, *Small*, 2012, **8**, 3073.
- 7 J. Park, S. Bauer, K. von der Mark and P. Schmuki, *Nano Lett.*, 2007, **7**, 1686.
- 8 S.-H. Oh, R. R. Finões, C. Daraio, L.-H. Chen and S. Jin, *Biomaterials*, 2005, **26**, 4938.
- 9 C. Das, P. Roy, M. Yang, H. Jha and P. Schmuki, *Nanoscale*, 2011, **3**, 3094.
- 10 S. Bauer, P. Schmuki, K. von der Mark and J. Park, *Prog. Mater. Sci.*, 2013, **58**, 261.
- 11 J.-W. Cheng, C. K. Tsang, F. Liang, H. Cheng and Y. Y. Li, *Phys. Status Solidi C*, 2011, **8**, 1812; H. Li, J. Zhang, J.-W. Cheng, Z. H. Chen, F. Liang, C. K. Tsang, H. Cheng, L. Zheng, S.-T. Lee and Y. Y. Li, *ECS J. Solid State Sci. Technol.*, 2012, **1**, M6.
- 12 J.-H. Ni, C. J. Frandsen, L.-H. Chen, Y.-Y. Zhang, J. Khamwannah, G. He, T.-T. Tang and S. Jin, *Adv. Eng. Mater.*, 2013, **15**, 464.

- 13 G. Loget, D. Zigah, L. Bouffier, N. Sojic and A. Kuhn, *Acc. Chem. Res.*, 2013, **46**, 2513; S. E. Fosdick, K. N. Knust, K. Scida and R. M. Crooks, *Angew. Chem. Int. Ed.*, 2013, **52**, 10438.
- 14 F. Mavr , K.-F. Chow, E. Sheridan, B.-Y. Chang, J. A. Crooks, R. M. Crooks, *Anal. Chem.*, 2009, **81**, 6218; F. Mavr , R. K. Anand, D. R. Laws, K.-F. Chow, B.-Y. Chang, J. A. Crooks and R. M. Crooks, *Anal. Chem.*, 2010, **82**, 8766.
- 15 J.-C. Bradley, H.-M. Chen, J. Crawford, J. Eckert, K. Ernazarova, T. Kurzeja, M. Lin, M. McGee, W. Nadler and S. G. Stephens, *Nature*, 1997, **389**, 268; G. Loget, J. Roche, E. Gianessi, L. Bouffier and A. Kuhn, *J. Am. Chem. Soc.*, 2012, **134**, 20033; J. Roche, G. Loget, D. Zigah, Z. Fattah, B. Goudeau, S. Arbault, L. Bouffier and A. Kuhn, *Chem. Sci.*, **5**, 1961.
- 16 G. Loget and A. Kuhn, *Nat. Commun.*, 2011, **2**, 535.
- 17 C. Ulrich, O. Andersson, L. Nyholm and F. Bj refors, *Angew. Chem. Int. Ed.*, 2008, **47**, 3034.
- 18 R. Ramaswamy and C. Shannon, *Langmuir*, 2010, **27**, 878; S. Ramakrishnan and C. Shannon, *Langmuir*, 2010, **26**, 4602.
- 19 S. Inagi, Y. Ishiguro, M. Atobe and T. Fuchigami, *Angew. Chem. Int. Ed.*, 2010, **49**, 10136.
- 20 S. So, K. Lee and P. Schmuki, *J. Am. Chem. Soc.*, 2012, **134**, 11316.
- 21 E. Gaul, *J. Chem. Educ.*, 1993, **70**, 176.
- 22 J. Duval, J. M. Kleijn and H. P. van Leeuwen, *J. Electroanal. Chem.*, 2001, **505**, 1; J. F. L. Duval, M. Minor, J. Cecilia and H. P. van Leeuwen, *J. Phys. Chem. B*, 2003, **107**, 4143;
- 23 A. J. Bard and L. R. Faulkner, *Electrochemical methods*, 2nd ed., John Wiley & Sons, Inc., 2001.